Shape recovery effect of 3D printed polymeric honeycomb : this paper studies the elastic behaviour of different honeycomb structures produced by PolyJet technology

Yap, Yee Ling; Yeong, Wai Yee

2015

Yap, Y. L., & Yeong, W. Y. (2015). Shape recovery effect of 3D printed polymeric honeycomb : this paper studies the elastic behaviour of different honeycomb structures produced by PolyJet technology. Virtual and Physical Prototyping, 10(2), 91-99. doi:10.1080/17452759.2015.1060350

https://hdl.handle.net/10356/143120

https://doi.org/10.1080/17452759.2015.1060350

Shape recovery effect of 3D printed polymeric honeycomb

Yap Y.L., Yeong W.Y.

Singapore Centre for 3D Printing, School of Mechanical & Aerospace Engineering, Nanyang Technological University, 50 Nanyang Avenue N3.1-B2c-03 Singapore 639798

Corresponding author. Tel.: +65-67904343; Email: WYYEONG@ntu.edu.sg

Abstract

Polymeric honeycombs, with their light-weight, high stiffness-to-weight ratio, and well-developed energy absorption characteristics, have been widely used in engineering applications. In this work, we report the shape recovery effect in a 3D inkjet-printed honeycomb core. Shape recovery effect, in which the honeycomb slowly recovers back to near its original shape, was observed after the release of compressive loading. Cyclic compression tests were carried out to study the shape recovery characteristics and factors affecting strain recovery in the 3D printed honeycombs. The factors such as honeycomb design shape, loading rate, and number of compression loading were investigated.. Flatwise compression tests were carried out on 3 different honeycomb shapes, namely hexagon, triangle, and circular, with three different loading rates. Three stages of shape recovery were identified and general conclusions on the factors affecting the shape recovery were proposed.

Keywords: 3D Printing, Inkjet printing, Honeycomb, Shape recovery effect

1. Introduction

Honeycomb sandwich structure has been an excellent innovation in composites industry due to its advantages on light weight, smooth skins and excellent fatigue resistance. It consists of two thin

facesheet materials attaching to an array of open cells, with typical hexagons or other cell configurations [1]. This structure is commonly used in applications ranging from sandwich panel for aircrafts, automobiles, building constructions to energy absorption, air directionalization, acoustic panels and light diffusion etc. Common polymeric honeycomb structures that are commercially available are made of polypropylene, polyurethane and polycarbonate [2]

Some groups have proposed variable shaped honeycomb using different fabrication technique such as thermoforming [3, 4], folding technique [5, 6], extrusion [7] and 3D printing [8, 9]. 3D printing or additive manufacturing presents a viable fabrication technique for advanced multi-functional honeycomb structures. As the honeycomb can be printed in a single process, further processing such as stacking and adhesive bonding are not required. This provides a faster manufacturing approach with reduced wastage of raw materials. Furthermore, the cellular design can be modified easily in the computer-aided environment thus creating the freedom in design that is not achievable in conventional manufacturing techniques. The honeycomb structure can be tailored to specific application and configuration. In this work, jetting technology or inkjet 3D printing was selected as the fabrication method.

Inkjet 3D printing technology has been utilized in many applications such as precision casting [10, 11], scaffold for tissue engineering [12] and prototypes fabrication [13, 14]., The advantages of inkjet printing are high precision, ease of use, rapid fabrication speed and wide range of materials available [15]. In this work, we report the shape recovery effect observed in a 3D inkjet-printed honeycomb core.

The shape recovery effect is a reversible elastic distortion when a material is elastically distorted. This phenomenon is also named as shape change effect (SCE) and is often observed in viscoelastic polymer, in which the material recovers back to its original shape gradually upon unloading, as shown in Figure 1 [16]. SCE is different from the shape memory effect (SME) as the shape memory materials require the presence of a particular stimulus, typically heat, chemical

and light, to recover the original (parent) shape [17]. Previous studies have reported this shape recovery phenomenon that the highly deformed and buckled polymeric honeycomb structure gradually recovered back to its original overall shape in hours upon unloading [18]. Notably, various polymer inks available in the commercial inkjet 3D printing system have been reported to possess thermally responsive shape memory effect [19].

Understanding and utilizing this shape recovery effect of polymeric honeycomb may present great advantages in some possible applications, for example, deployable space structures [20]. This paper therefore aims to investigate the factors affecting the shape recovery behavior of polymeric honeycombs, which include cell shapes of honeycomb, loading rates.

2. Specimen preparation and experiments

2.1. Design of honeycomb structure

Three basic designs of honeycomb structure, namely hexagon, triangle, and circular, were used in this experiment to examine the effect of different honeycomb shapes on the shape recovery. Figure 2 shows the 3 honeycomb structures configurations, with a dimension of 60mm x 60mm x 10mm. Relative density of the honeycomb has been identified as one of the dominant factors that affects the mechanical properties of the honeycomb [21]. The specimens were hence designed to have constant relative density of 20% to remove the effects of relative density and to investigate only the shape recovery effect of different honeycomb cell shape. The specimen height was designed to be 10mm while the cell wall thickness is fixed at 0.6mm for all 3 configurations.

2.2. Specimen Fabrication and Preparation

The specimens of polymer honeycomb were fabricated using polypropylene-like materials, DurusWhite (RGD430) with PolyJet system, Objet500 Connex3. PolyJet 3D inkjet printing technology developed by Objet features 16-micron layers with accuracy up to 0.2 mm for smooth surfaces, thin walls and complex geometries, which is suitable for manufacturing honeycomb

structures [22]. PolyJet print heads jet layers of UV curable liquid photopolymer onto build tray and the UV light immediately cures the resin to form a fully polymerized object layer by layer [15].

After printing was completed, the specimens were cleaned to remove the support material. The post-processed specimens are shown in Figure 3.

2.3. Mechanical experiment

The flatwise compressive experiments were performed on specimens with different cell design and material, and were subjected to different loading rate as listed in Table 1. The specimens were further subjected to compression at 0.5mm/min loading rate. The conventions for labelling specimens for each factor were also included in the parentheses in Table 1. The flatwise compression tests were conducted based on the ASTM C365/C365M-11a [23] using an Instron 5500R universal testing machine with a load cell of 50kN. The strain measurement was taken directly from the crosshead displacement. All experiments were conducted in the air-conditioned lab with temperature and humidity maintained at 22℃ and 55%, respectively, to minimize the effect of thermal expansion. The initial height of honeycomb core was measured before the testing, using micrometer. Figure 4a and Figure 4b show an image of the specimen under compression and the schematic of experimental arrangement of the honeycomb flatwise compression experiments, respectively.

Upon unloading, the specimen's height was recorded immediately as well as after a period of 1, 2, 3, 4, 5, 15, 30, 60 minutes and 1 day. At least two measurements were conducted at random node position on the honeycomb using a micrometer.

After 2 days upon unloading from the first compression, the honeycomb core was noticed to have recovered to its maximum achievable height. Hence the second compression loading was performed only after 2 days of the initial experiment. Fig. 4a-4f show the significant recovery

stages in a selected DurusWhite circular honeycomb specimen: before compression (Fig 4a), immediate upon unloading (Fig 4b), 5 minutes after unloading (Figure 4c), 1 hour after unloading (Figure 4d), 1 day after unloading of the 1st compression (Figure 4e), 1 day after unloading of the 2nd compression (Figure 4f). The DurusWhite specimen showed extensive deformation due to compression load as the honeycomb specimen was crushed to 50% strain. After unloaded to zero load, the honeycomb specimen experienced very rapid recovery during the first hour. The specimen was near-full shape recovery after 1 day. Faster crack propagation as well as fracture were observed in the following compression test conducted two days later.

3. Results and discussion

3.1. Compression Stress-strain Curve and Maximum Stress

Figure 6 shows a typical stress-strain curve obtained from the flatwise compressive tests for honeycomb structures. The compressive stress increases linearly with strain attributed to the elastic bending of the cell walls. The core yielded at approximately 80% of its maximum strength.

Effect of loading rate: In terms of loading rate, from Fig. 7 it is observed that the ultimate compressive strength of the honeycombs increases with loading rate. This could be due to the larger resistance force resulting from faster loading.

Effect of honeycomb design: Circular honeycomb has the highest compressive strength of 6.82 MPa. The average compressive strength of hexagonal and triangular honeycombs was found to be 4.54 MPa and 2.52 MPa respectively. It is noted that the ultimate compressive strength increases as the number of sides of the polygon increases from 3-sided triangle to 6-sided hexagon and until the polygon finally develops into a circle. The trend of the out-of-plane compressive properties in different cell shapes were also reported in previous literature [24].

Effect of 2nd loading test: Figure 9 shows the ultimate compressive strength of the second compressive loading. The specimens after the second loading generally have lower compressive

strength compared to their first loadings. The maximum compression strength reduces by an average of 26.6% due to plastic deformation during the first compression loading.

3.2 The Shape Change Effect (SCE)

To normalize the effect of difference in original thickness due to 3D printing limitation on accuracy, the percentage height ($h/h_0*100\%$) was adopted in the analysis [25]. The percentage height-time graph was plotted for selected specimens to analyze the strain recovery rate, as shown in Figure 10.

It is observed that all the specimens recovered to more than 60% of their original height in the first 5 minutes, and most of the specimens recovered more than 80% after 1 hour of unloading from 50% strain. Afterwards, the recovery rate declined sharply and the recovery of shape was recorded after 23 hours, which is 1 day after unloading. The specimens were able to recover to their original shapes and height gradually by about 5% over this period of time.

The shape recovery can be classified into 3 stages, as indicated in Figure 10. Stage 1 is defined as rapid recovery stage for the first 5 minutes upon immediate unloading after the specimen was crushed to 50% strain. The elastic deformation was quickly recovered in this stage. This is evident from the honeycomb on average recovered to about 70% thickness almost instantaneously upon unloading from 50% strain. Stage 2 was marked as the transition stage, for the next 55 minutes after Stage 1, in which the honeycomb recovered in a decreasing rate, from 9.4% in the first 5 minutes in Stage 1 to 7% in 55 minutes in the Stage 2. Most of honeycomb regained nearly 85 to 90% of its original height at the end of Stage 2. Lastly, Stage 3 was identified as equilibrium stage from the second hour to 1 day after unloading, in which the honeycomb expanded to its original shape in an even slower rate at about 5%.

The shape recovery effect of polymeric honeycomb could be owing to the natural viscoelasticity that general polymers have; their elastic deformation is recovered slowly after being compressed.

From the literature review on superelasticity of semicrystalline polymers such as syndiotactic polypropylene (sPP) [26], phase transition occurs during large tensile deformation and release of the deformation, suggesting phase change as a possible mechanism of shape change effect in polymers. However, further research is still necessary to understand in depth the mechanism.

3.3 Effect of Honeycomb Design Shape

Figure 11 shows the SCE response of the selected specimens DH2, DT2 and DC2. It is observed that the 3 different design shapes had almost the same initial percentage thickness immediately after compression (Stage 1), but triangle honeycomb recovered slightly faster than hexagon honeycomb, and circular honeycomb recovered the slowest. In terms of the final recorded height percentage, triangular honeycomb was able to recover back to slightly higher percentage than both hexagon and circular honeycomb. This trend is the opposite with the strength of different honeycomb shapes, implying that shape recovery has an inverse relationship with the strength of the honeycomb configuration.

3.4 Effect of Loading Rate

The loading rate also affects the shape recovery response on honeycomb. Figure 12 shows the shape recovery response of the specimens DT1, DT2 and DT3 with different loading rates. It can be seen that with increase in loading rate, the immediate percentage thickness increases as well, showing a stronger strain recovery in stage 1. The specimens continued to expand to almost similar height till 1 day later, where the recovery rate is slightly higher in stage 2 and 3 for specimens subjected to lower compressive loading rate. This phenomenon could be due to the energy stored during slow loading is larger than that in fast loading, resulting in a slower recovery response in stage 1. Nevertheless, all the samples eventually reached the equivalent energy level and returned to similar height.

3.6 Effect of Second Loading

Figure 13 shows the shape recovery response of the 1st and 2nd loading for the specimen DT2 and DT*, It is observed that the recovery rate for 2nd loading is slightly faster and higher than the 1st loading. This phenomenon could be owing to the reduced strength and stiffness of the structure after two loadings.

3.7 2-day Near-full Recovery

The experiment data has also proven the assumption of 2-day near-full recovery for the samples to carry on with 2nd loading. The height recovery from day 1 to day 2 is only 0.52% on average, implying the near-full recovery after day 2. The near-full recovery for DurusWhite honeycomb is 99.57% on average, as shown in Table 2.

4. Conclusions

This paper identified the stages and analyzed the factors affecting the shape recovery of polymer honeycomb, which was fabricated using 3D inkjet printing technology. Following are the conclusions:

- In terms of loading rate, the maximum compressive strength increases as the loading rate increases, and the initial thickness after compression increases, indicating a strong recovery rate in stage 1. However, the final honeycomb heights after stage 3 are comparable, regardless of the loading rate.
- In terms of honeycomb design shape, circular honeycomb has the highest strength, followed by hexagonal and triangular honeycomb. The ultimate compressive strength increases with the number of sides in the polygonal cell shape. The triangular

honeycomb, nevertheless, has a faster recovery rate than hexagonal and circular honeycomb, suggesting an inversed relation between strength and strain recovery.

- Comparing the 2nd loading to the 1st loading, as the specimens have undergone the first cycle of deformation, the original stiffness is much weakened, leading to lower compressive strength in the 2nd loading. This also led to a stronger recovery rate upon unloading after the 2nd loading.

The findings have broad potential implications for lightweight polymer honeycomb energy absorption materials, compliance-matched biomedical implants and smart/adaptive structures.

Acknowledgments

This project is funded under A*STAR TSRP - Industrial Additive Manufacturing Programme by A*STAR Science & Engineering Research Council (SERC).

References

[1] T. Bitzer, *Honeycomb Technology [electronic resource] : Materials, Design, Manufacturing, Applications and Testing / by Tom Bitzer*: Dordrecht : Springer Netherlands : Imprint: Springer, 1997., 1997.

[2] R. Stewart, "At the core of lightweight composites," *Reinforced Plastics,* vol. 53, pp. 30-35, 4// 2009.

[3] J. Pflug and I. Verpoest, "Thermoplastic folded honeycomb structure and method for the production thereof," 2004.

[4] J. Philipp Bratfisch, D. Vandepitte, J. Pflug, and I. Verpoest, "Development and Validation of A Continuous Production Concept for Thermoplastic Honeycomb," in *Sandwich Structures 7: Advancing with Sandwich Structures and Materials*, O. T. Thomsen, E. Bozhevolnaya, and A. Lyckegaard, Eds., ed: Springer Netherlands, 2005, pp. 763-772.

[5] S. Fischer, K. Drechsler, S. Kilchert, and A. Johnson, "Mechanical tests for foldcore base material properties," *Composites Part A: Applied Science and Manufacturing,* vol. 40, pp. 1941-1952, 12// 2009.

[6] Y. Hou, R. Neville, F. Scarpa, C. Remillat, B. Gu, and M. Ruzzene, "Graded conventional-auxetic Kirigami sandwich structures: Flatwise compression and edgewise loading," *Composites Part B: Engineering,* vol. 59, pp. 33-42, 2014.

[7] J. Bournazel and G. Ducruy, "Method and applications for the extrusion of thermoplastic honeycomb structure, and structures thus obtained," 1987.

[8] Y. Hou, Y. H. Tai, C. Lira, F. Scarpa, J. R. Yates, and B. Gu, "The bending and failure of sandwich structures with auxetic gradient cellular cores," *Composites Part A: Applied Science and Manufacturing,* vol. 49, pp. 119-131, 2013.

[9] J. V. Nygaard and A. Lyckegaard, "Sandwich Beam with a Periodical and Graded Core Manufactured Using Rapid Prototyping," *Journal of Sandwich Structures and Materials,* vol. 9, pp. 365-376, 2007.

[10] R. Singh, V. Singh, and M. S. Saini, "Experimental investigations for statistically controlled rapid moulding solution of plastics using polyjet printing," pp. 1049-1053.

[11] C. M. Cheah, C. K. Chua, C. W. Lee, C. Feng, and K. Totong, "Rapid prototyping and tooling techniques: a review of applications for rapid investment casting," *The International Journal of Advanced Manufacturing Technology,* vol. 25, pp. 308-320, 2004.

[12] W.-Y. Yeong, C.-K. Chua, K.-F. Leong, M. Chandrasekaran, and M.-W. Lee, "Development of scaffolds for tissue engineering using a 3D inkjet model maker," p. 115.

[13] M. Salmi, K. S. Paloheimo, J. Tuomi, J. Wolff, and A. Makitie, "Accuracy of medical models made by additive manufacturing (rapid manufacturing)," *J Craniomaxillofac Surg,* vol. 41, pp. 603-9, Oct 2013.

[14] D. Ibrahim, T. L. Broilo, C. Heitz, M. G. de Oliveira, H. W. de Oliveira, S. M. Nobre*, et al.*, "Dimensional error of selective laser sintering, three-dimensional printing and PolyJet models in the reproduction of mandibular anatomy," *J Craniomaxillofac Surg,* vol. 37, pp. 167-73, Apr 2009.

[15] C. K. Chua and K. F. Leong, *3D Printing and Additive Manufacturing: Principles and Applications Fourth Edition of Rapid Protoyping*, 4th ed.: World Scientific, 2014.

[16] X. Wu, W. Huang, Y. Zhao, Z. Ding, C. Tang, and J. Zhang, "Mechanisms of the Shape Memory Effect in Polymeric Materials," *Polymers,* vol. 5, pp. 1169-1202, 2013.

[17] L. Sun, W. M. Huang, Z. Ding, Y. Zhao, C. C. Wang, H. Purnawali*, et al.*, "Stimulus-responsive shape memory materials: A review," *Materials & Design,* vol. 33, pp. 577-640, 1// 2012.

[18] H. X. Zhu and N. J. Mills, "The in-plane non-linear compression of regular honeycombs," *International Journal of Solids and Structures,* vol. 37, pp. 1931-1949, 3// 2000.

[19] K. Yu, A. Ritchie, Y. Mao, M. L. Dunn, and H. J. Qi, "Controlled Sequential Shape Changing Components by 3D Printing of Shape Memory Polymer Multimaterials," *Procedia IUTAM,* vol. 12, pp. 193-203, // 2015.

[20] U. Maheshwaraa Namasivayam and C. Conner Seepersad, "Topology design and freeform fabrication of deployable structures with lattice skins," *Rapid Prototyping Journal,* vol. 17, pp. 5-16, 2011.

[21] L. J. Gibson and M. F. Ashby, *Cellular solids : structure and properties*: Cambridge ; New York : Cambridge University Press, 1997.

2nd ed., 1997.

[22] Stratasys. *PolyJet Technology*. Available: http://www.stratasys.com/3d-printers/technologies/polyjet-technology

[23] A. International, "ASTM C365 / C365M-11a, Standard Test Method for Flatwise Compressive Properties of Sandwich Cores," ed. www.astm.org, 2011.

[24] Y. L. Yap, Y. M. Lai, H. F. Zhou, and W. Y. Yeong, "Compressive strength of thin-walled cellular core by inkjet-based additive manufacturing," presented at the Proceedings of the 1st International Conference on Progress in Additive Manufacturing, Singapore, 2014.

[25] K. McCarthy, "Improving Rapid Prototyping Through the Installment of 3D Printers in Automotive Companies," Paper Engineering, Chemical Engineering and Imaging (to 2013), Western Michigan University, Honors Theses, 2012.

[26] F. Auriemma, C. De Rosa, S. Esposito, and G. R. Mitchell, "Polymorphic Superelasticity in Semicrystalline Polymers," *Angewandte Chemie International Edition,* vol. 46, pp. 4325-4328, 2007.

Table 1: Factors of investigation in the out-of-plane compression experiments

Material	DurusWhite RGD430 (D)
Honeycomb cell shape (with constant relative density)	Circle (C) Triangle (T) Hexagon (H)
Loading rate (mm/min)	0.25 (1) 0.50 (2) 1 .00(3)
Second loading at the same rate (mm/min) (after the parts have recovered to maximum)	0.50 (*)

Table 2: Near-full recovery before 2nd loading

	Initial Thickness (mm)	Day 1	Day 2	% increase from day 1 to day 2 after compression	day 2/initial
DH2	10.04	9.95	10.00	0.50%	99.60%
DT2	10.06	10.04	10.05	0.15%	99.90%
DC2	10.07	9.90	9.99	0.91%	99.21%
			Average	0.52%	99.57%

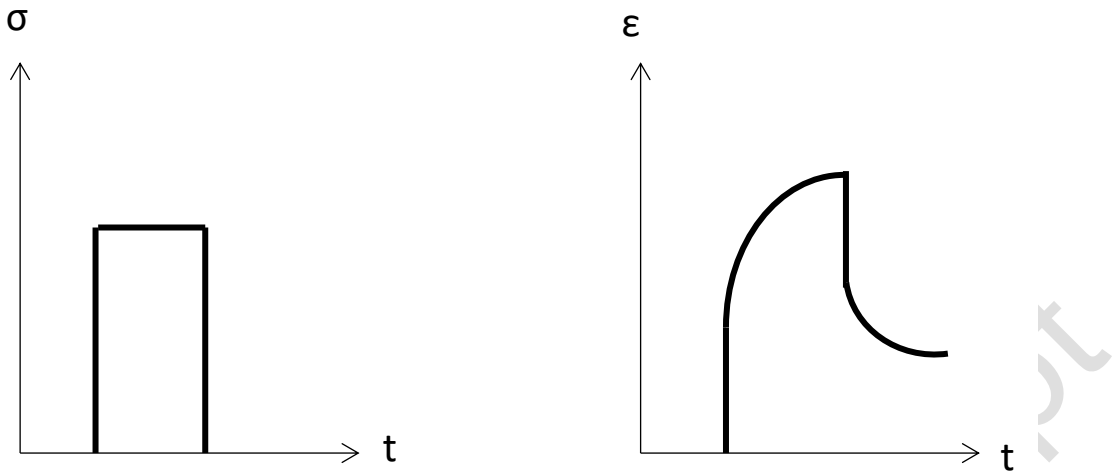

Figure 1: Viscoelastic effect of stress and strain against time

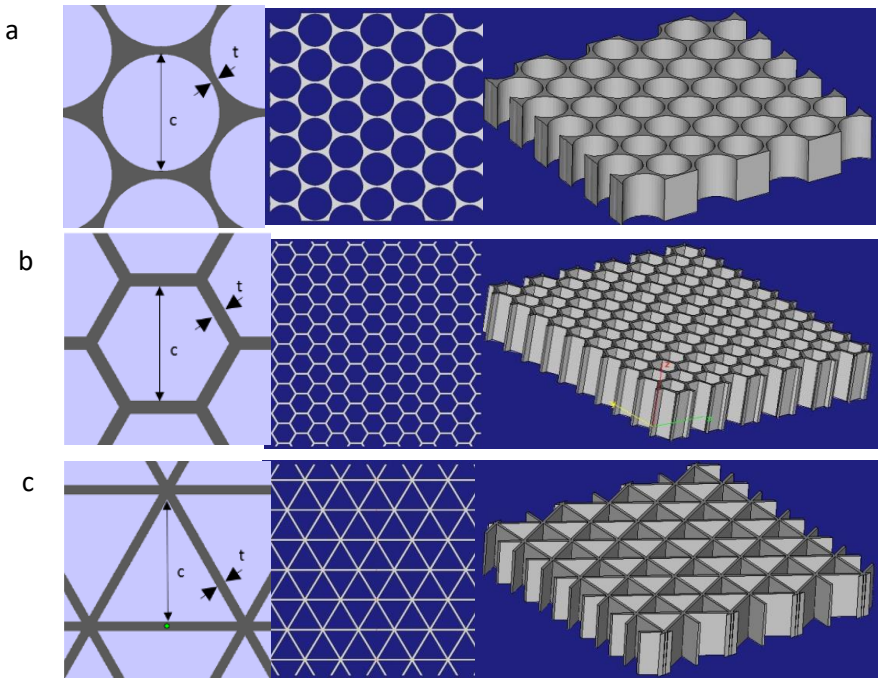

Figure 2: 3 Unit cell, top view and isometric view of each honeycomb structure configurations: (a) Circular (c=9.8mm, t=0.6mm), (b) Hexagon (c=3.125mm, t=0.6mm), and (c) Triangle (c=9.14mm, t=0.6mm)

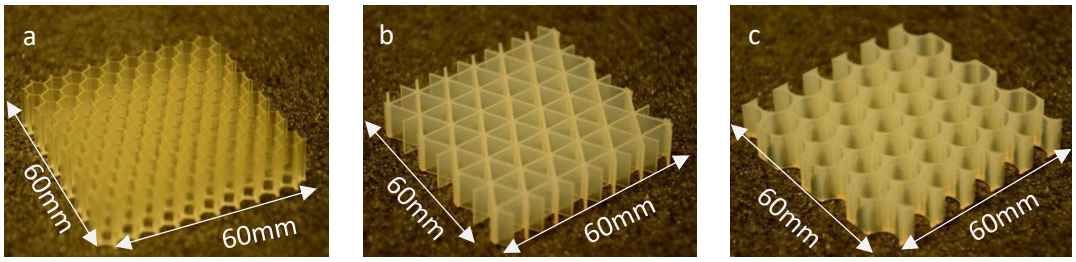

Figure 3: 3D Printed honeycomb specimens: (a) hexagonal honeycomb, (b) triangular honeycomb and (c) circular honeycomb

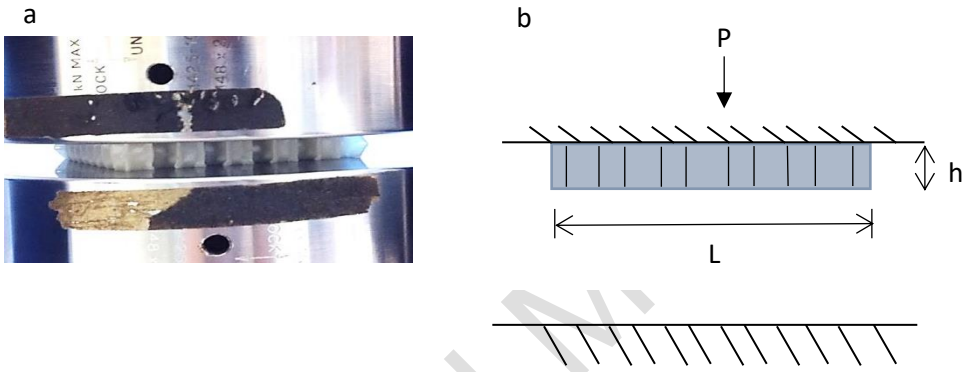

Figure 4: Experimental arrangement: (a) specimen image during testing and (b) schematic of honeycomb flatwise compression experiments

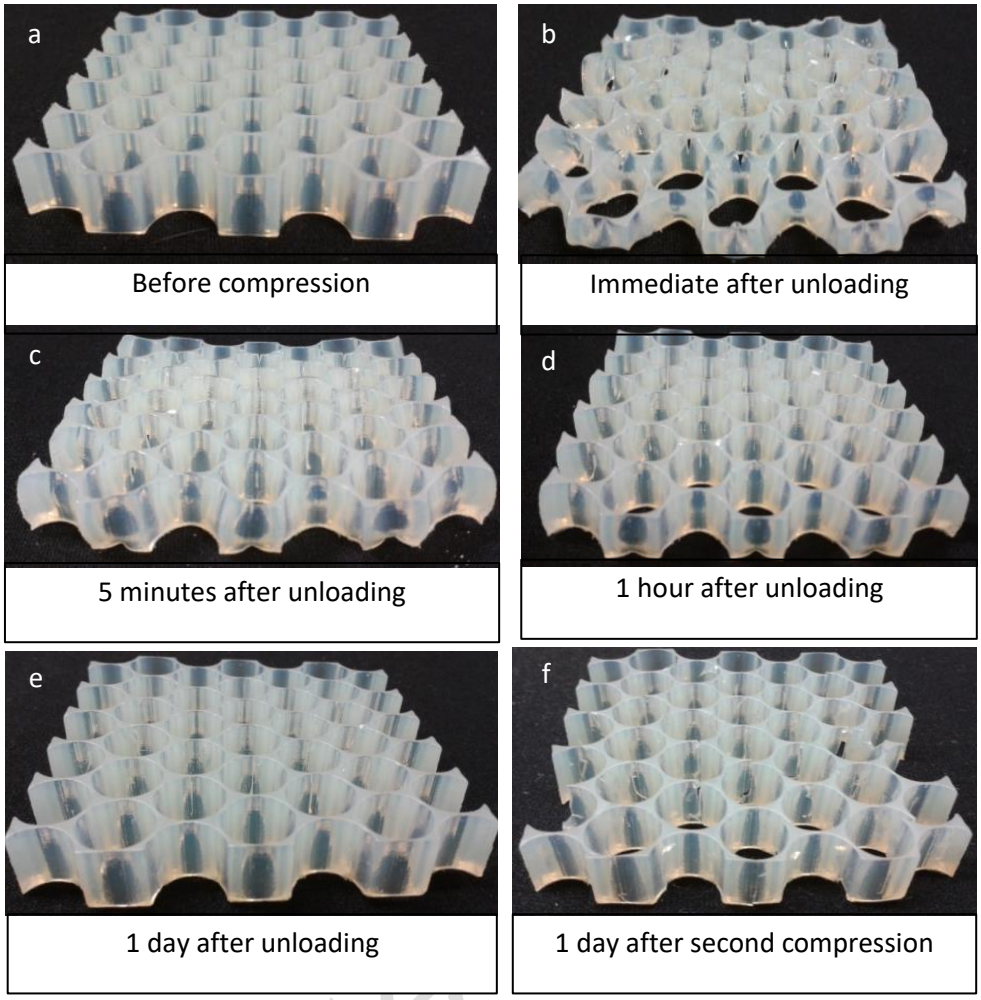

Figure 5: Images of shape recovery process of a selected DurusWhite circular honeycomb specimen: (a) before compression, (b) immediate upon unloading , (c) 5 minutes after unloading, (d) 1 hour after unloading, (e) 1 day after unloading, (f) 1 day after unloading of the second compression

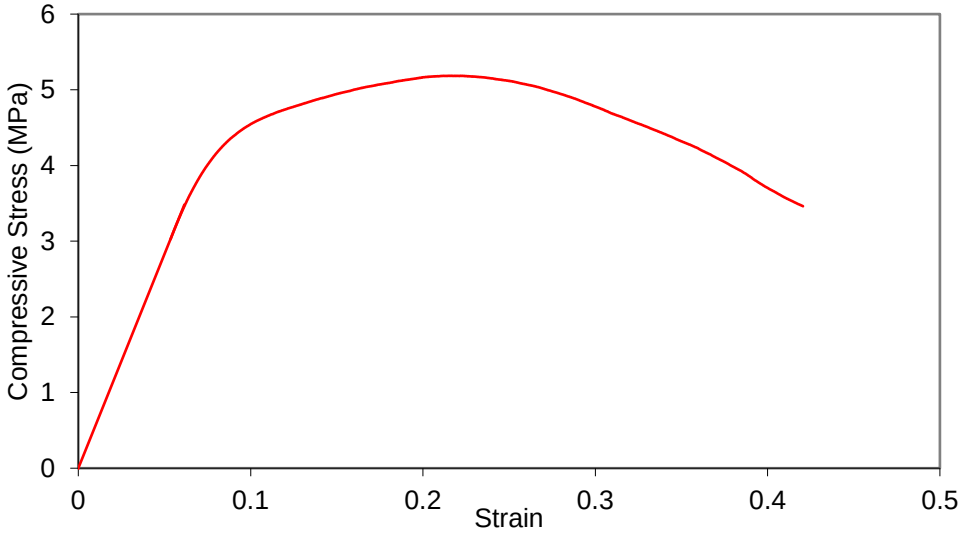

Figure 6: Stress-strain curve of a typical honeycomb specimen

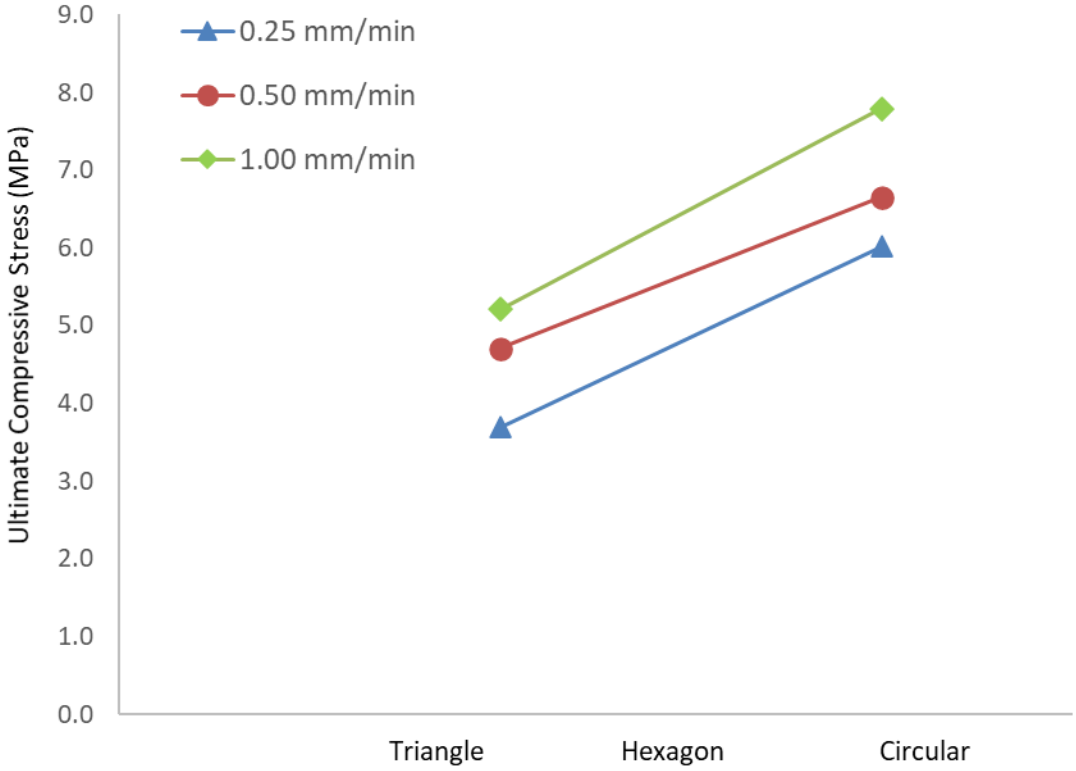

Figure 7: Effects of loading rate on the ultimate compressive strength of the honeycombs

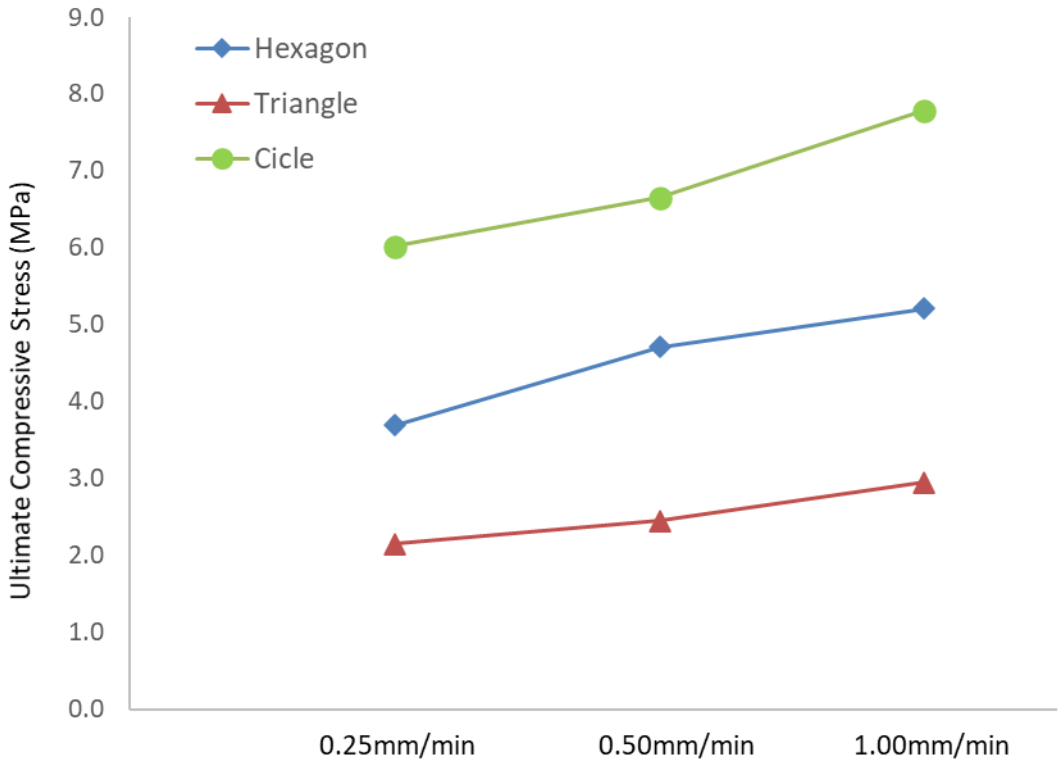

Figure 8: Effects of honeycomb cell shapes on the ultimate compressive strength of the honeycombs

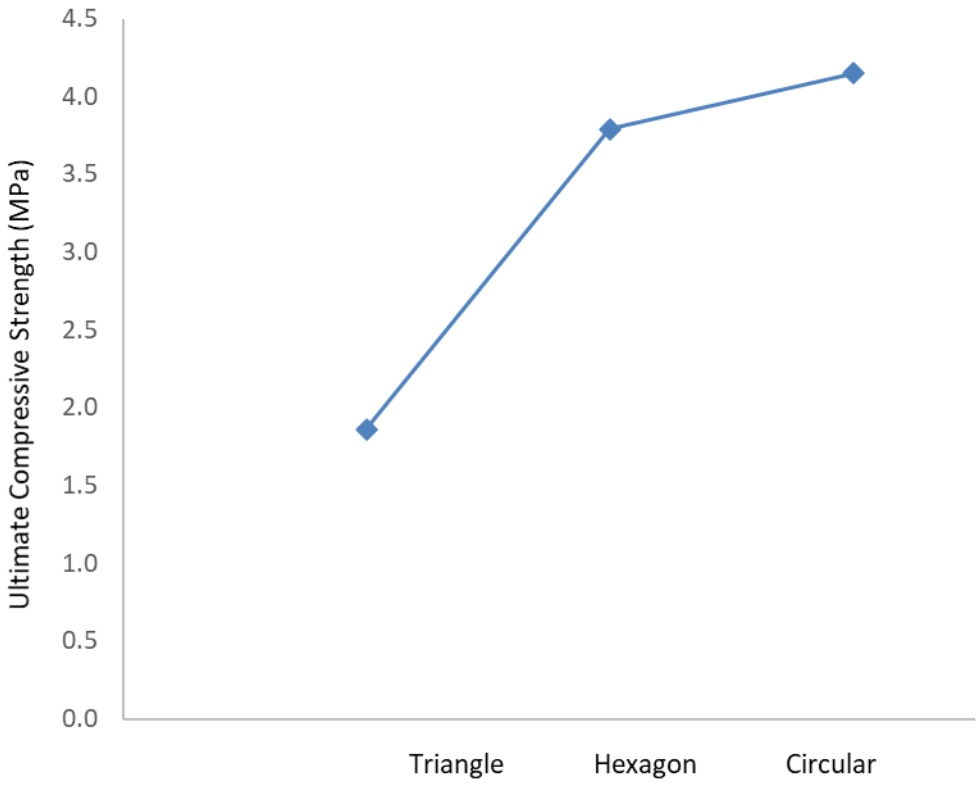

Figure 9: Ultimate compressive strength of honeycombs after second compression

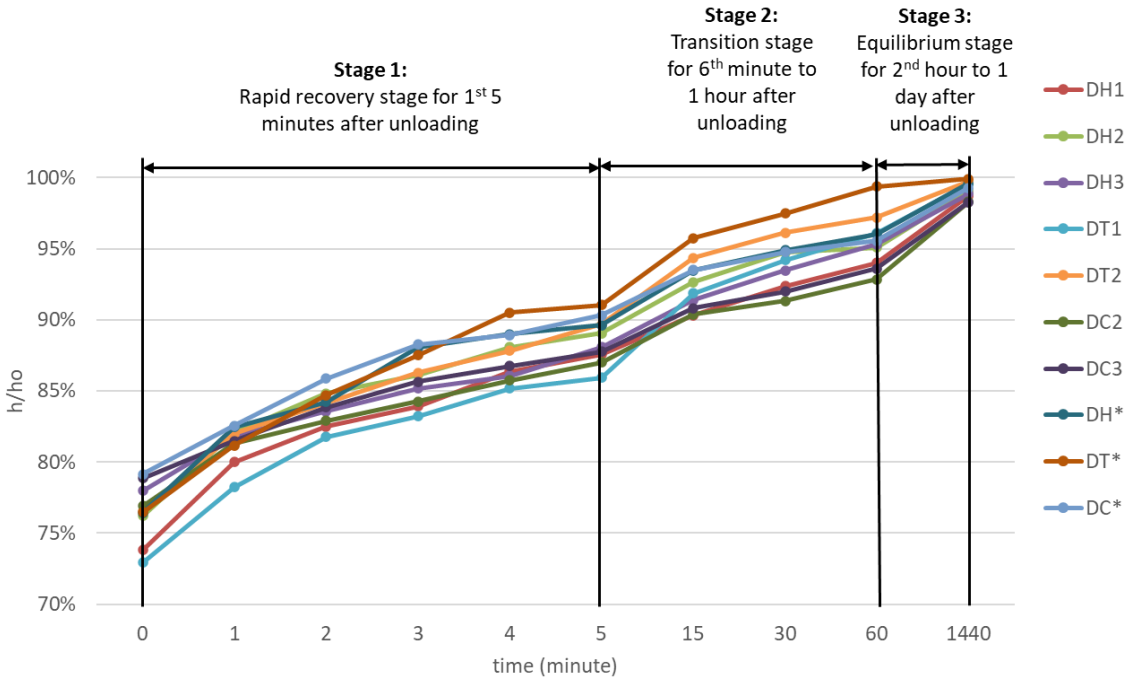

Figure 10: Shape recovery rate of the honeycombs in 3 stages (time scale is modified for each stage for better illustration of the recovery rate)

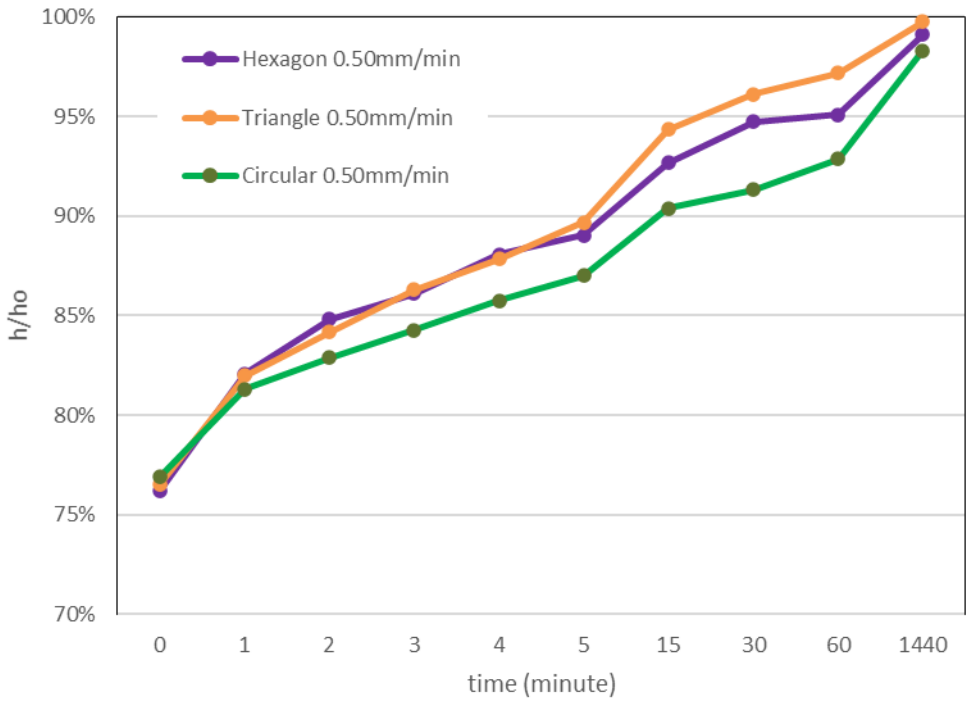

Figure 11: Shape recovery rate of 3 specimens with different cell shape at 0.50 mm/min loading rate

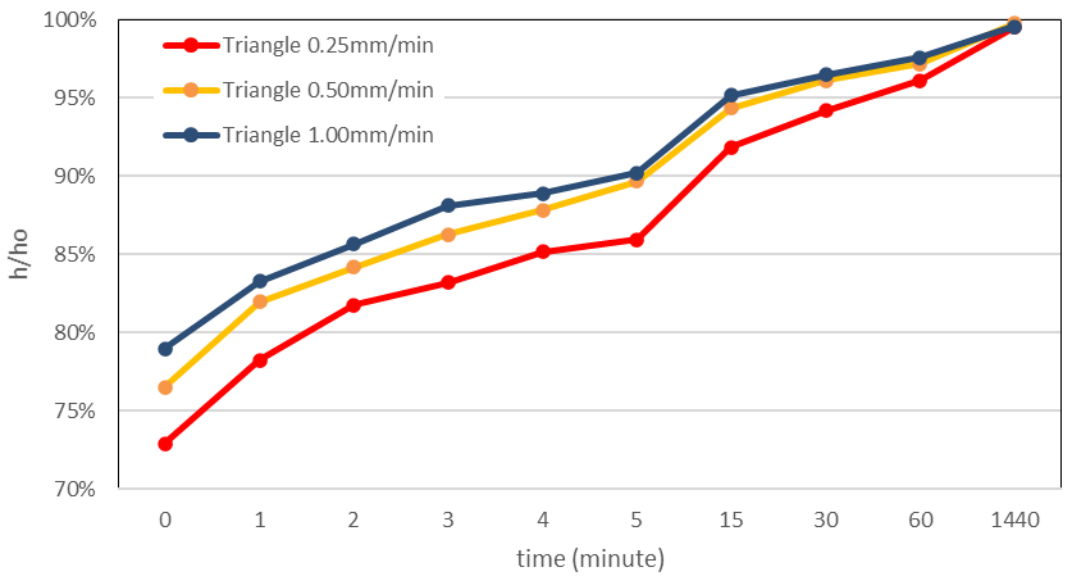

Figure 12: Shape recovery rate of the triangular honeycombs of different loading rates

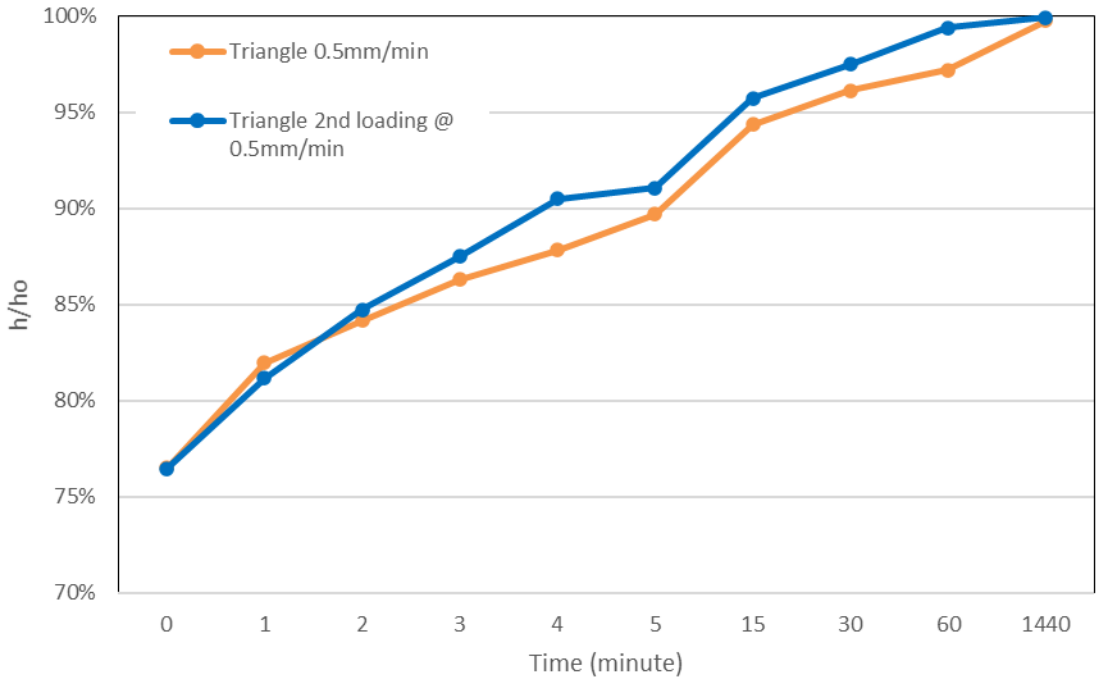

Figure 13: Comparison of shape recovery rate for first and second loading